International Journal of Engineering Trends and Technology
ISSN: 2231–5381 / https://doi.org/10.14445/22315381/IJETT-V72I3P118

Volume 72 Issue 3, 193-207, March 2024

Original Article

Study on Ductile-To-Brittle Transition Behavior in Fixed Diamond Abrasive Wire Sawing Process of Monocrystalline Silicon Ingot

Quoc-Phong Pham[1], Le Ngoc Quynh Hoa[2], Muhamad Amirul Haq[3], Le Nam Quoc Huy[4]

[1]*School of Engineering and Technology, Tra Vinh University, Tra Vinh, Vietnam.*
[2]*Emerging nanoscience Research Institute (EnRI), Nanyang Technological University, Singapore.*
[3]*Department of Computer Science, Muhammadiyah University of Surabaya, Indonesia.*
[4]*Department of Mechanical Engineering, National Taiwan University of Science and Technology, Taiwan.*

[1]*Corresponding Author : phongpham@tvu.edu.vn*

Received: 25 October 2023 Revised: 09 February 2024 Accepted: 22 February 2024 Published: 17 March 2024

Abstract *- Monocrystalline silicon has become one of the most popular semiconductor materials for diverse industrial applications on account of its exceptional physical. As one of the initial steps of the monocrystalline silicon wafer manufacturing process, fixed diamond abrasive wire sawing is widely used in the slicing process because it provides faster, cleaner, increased size of the ingot as well as decreased the sawn kerf loss when compared with slurry wire sawing process. However, challenges arise from monocrystalline silicon's intrinsic hardness and brittleness, often resulting in subsurface cracks and micro-cracks on the surfaces of as-sawn wafers. To overcome these obstacles, this study employed a ductile regime machining technique applied to the fixed diamond abrasive wire sawing process. Moreover, this study calibrated accurately specific cutting energy consumption to remove material in ductile mode at the ductile to brittle transition point, which is used as a reference value for optimizing experimental parameters during the verification process. The findings of this study not only enhance our understanding of the mechanism behind the removal of brittle materials in a ductile manner but also serve as an experimental benchmark for achieving crack-free and subsurface damage-free monocrystalline silicon wafers through fixed diamond abrasive wire sawing processes.*

Keywords *- Specific cutting energy, Scratching experiment, Ductile-brittle transition, As-sawn wafer surface morphology, Fixed diamond abrasive wire sawing process, Monocrystalline silicon.*

1. Introduction

As the global community increasingly directs its attention towards sustainable energy solutions, solar cell technology remains at the forefront of these discussions. Central to this solution is monocrystalline silicon, lauded for its superior photoelectric properties and its potential to significantly reduce carbon emissions originating from fossil fuel utilization [1-3]. The manufacturing process is a crucial factor in determining the quality of solar cell products, and sawing ingot plays an important role in the manufacturing procedures; as the first stage of semiconductor wafer production, it significantly influences the quality of the wafer throughout later manufacturing procedures. [4, 5]. In recent years, fixed diamond abrasive sawing processes have been developed for the sawing process of monocrystalline silicon ingot as a result of a number of potential benefits, including the possibility of expediting the sawing process, cost-effectiveness, reducing kerf loss, and an environmentally conscious approach, especially when compared to conventional slurry sawing techniques [6-7]. However, due to the high brittleness mechanical characteristics of monocrystalline silicon material, the as-sawn wafer's surface topography is more prone to brittle fracture than plastic deformation as the material removal mechanism in the process of fixed diamond abrasive wire sawing Therefore, a ductile removal mode must be obtained via a fixed diamond abrasive wire sawing process in order to ensure that the as-sawn wafer's surface topography and subsurface are free of cracks [8-10].The ductile-regime machining technique is one of the methods used to enhance the surface quality of brittle materials in precision manufacturing. It has been specifically designed to provide good outcomes in creating semiconductor materials [11-14]. The results of these studies have demonstrated that ductile-regime machining can be used to manufacture semiconductor materials and ceramic materials to remove the material by plastic flow and minimize the effects of brittle fractures on the surface morphology [15, 16].

Giovanola et al. performed research which revealed that brittle materials may be effectively removed using a modest cutting depth, resulting in a ductile-regime manner of material removal [17]. Puttick et al. and Venkatachalam et al. found that there exists a ductile–brittle transitional point at which a material transitions from being ductile to brittle. Below this point, the brittle material may be removed in a plastic manner without creating any cracks on the machined surface. [18, 19].

In order to enhance the quality of as-sawn wafers made from brittle semiconductor materials by the use of the ductile mode, a number of studies have been undertaken to examine the impact of sawing parameters on the surface of as-sawn wafer's surface throughout the fixed diamond abrasive wire process. According to the research by Suzuki et al., the transition from brittle to ductile mode is influenced by diamond grit size during the fixed diamond abrasive wire sawing process [20]. Upon analyzing the chip shape after the sawing process, it is possible to determine the transition from ductile to brittle silicon. The study conducted by Gao et al. on the fixed diamond abrasive sawing process of monocrystalline silicon shows that increasing wire speed and decreasing feed speed during the sawing process can improve the surface roughness and subsurface damage of as-sawn wafers [21]. In a recent study, Wang et al. proposed a numerical model that predicts the depth of the subsurface damage caused by fixed diamond abrasive wire sawing based on the mechanics of indentation fractures [22]. The results of the study indicate that there is a critical ratio between the feed velocity and the wire velocity in the sawing process, which could allow the removal of the material in ductile mode. Wang et al. and Hardin et al. studied the effect of abrasive distribution, shape, and characteristics on as-sawn wafer quality, as well as the link between cutting force and surface roughness throughout the sawing process. [23, 24].

According to the results of the studies outlined above, the ingots are sliced using a reciprocal fixed diamond abrasive wire sawing process, with particular attention paid to the impact of each process parameter on the quality of the as-sawn wafers.

Additionally, these methods required significant expenditures due to the numerous experimental procedures conducted, as well as a limitation of these studies is the difficulty of applying these study results to other materials, different sawing machines, or fixed diamond abrasive wires with different properties.

In order to address these obstacles, it is critical to precisely ascertain the position at which the material removal mechanism transitions from a ductile to a brittle state. Therefore, in this study, the ductile-to-brittle transitional point is determined based on signal analysis of tangential force and coefficient from a scratching experiment using a single diamond on monocrystalline silicon in combination with image analysis using a scanning electron microscope (SEM) to confirm the exact position.

Moreover, the calibration-specific cutting energy at the ductile-to-brittle transition point is utilized as a criterion for estimating the energy that is consumed for removing the material of unit volume of monocrystalline silicon material and then validated of fixed diamond wire sawing experimental based on specific cutting energy data at transitional point applied for plastic deformations as estimates based on as-sawn wafer surface quality. By implementing the concept of specific cutting energy associated with the material removal mechanism in the ductile-regime technique, this research aims to enhance the sawing process by reducing energy consumption and improving the quality of the as-sawn wafer.

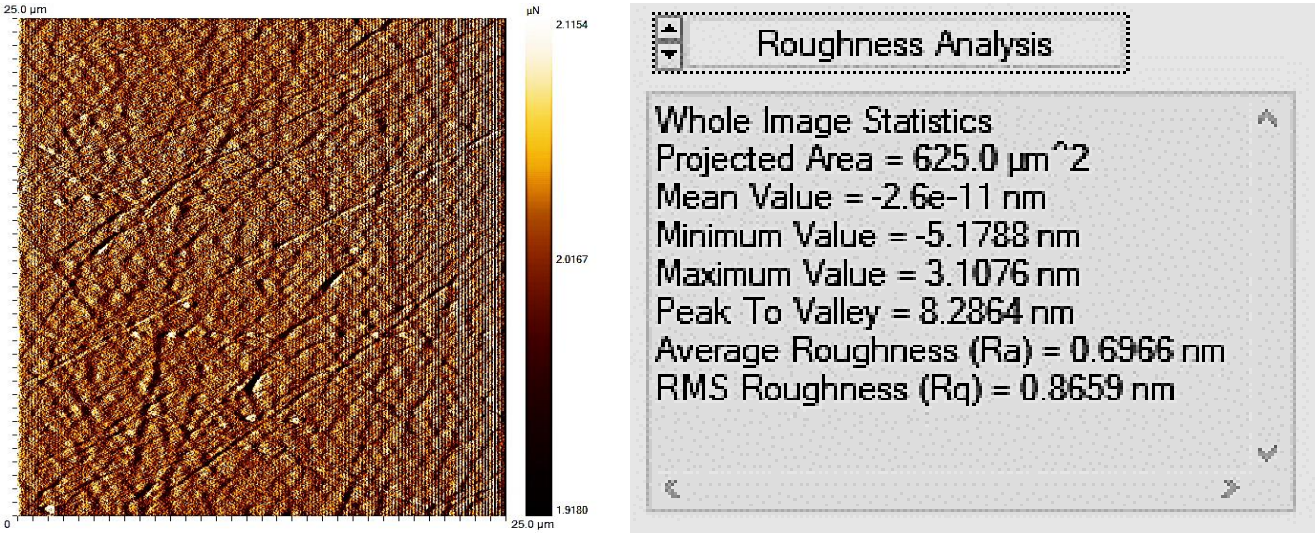

Fig. 1 Analyzing the surface characteristics of monocrystalline silicon workpiece after chemical mechanical polishing with AFM measurement instrument

2. Ductile-to-Brittle Transition

2.1. Sample preparation

In order to prepare the monocrystalline silicon workpieces for the scratching experiment and fixed abrasive wire sawing processes, the commercially available 4-inch monocrystalline silicon ingot is sliced into two cubic workpieces with the same identical dimensions of 3 cm x 3 cm x 3 cm as part of the preparation sample process for the scratching test of the monocrystalline silicon workpiece in Section 2.2. It is necessary to chemically mechanically polish the surface of a monocrystalline silicon workpiece to eliminate surface defects.

Chemical mechanical planarization is performed using the Logitech PM5 polisher (Logitech, Glasgow, Scotland) in conjunction with IC1000 polishing pad (IC1000, Dow Chemical Company, Michigan, USA) and PlanerLite 6000 polishing solution (Fujimi, Kiyosu, Japan) to polish monocrystalline silicon workpiece on crystallographic orientation (100). To minimize the effect of surface roughness on scratching experiment results, a monocrystalline silicon workpiece is polished to achieve a surface roughness of less than 2 nm. The atomic force microscope (AFM) measurement instrument is then utilized to examine the surface roughness of polished workpieces, as illustrated in Figure 1.

2.2. Determination of the Ductile-to-Brittle Transition

The objective of this section is to ascertain the transitional phase between the ductile and brittle modes of a monocrystalline silicon workpiece through a scratching experiment, which is carried out on the high-load option of the nano-triboindenter instrument (Hysitron TI 950, Burker Inc, Minneapolis, USA). The conical diamond-shaped with a radius of 5 µm and cone angle of 60^0 is used for the scratching experiment; it is performed on the polished surface (100) of a monocrystalline silicon workpiece along the crystallographic direction <011>.

Moreover, the ramp load function is implemented by linearly increasing the normal force from 0 to 350 milliNewtons (mN) with a scratching length of 250 micrometers for the purpose of experimentation. The micrograph images of the groove from the scratching experiment are observed using a scanning electron microscope instrument, as shown in Figure 2.

Based on the SEM micrograph images, three distinct stages of the material removal mechanism during the scratching procedure of the monocrystalline silicon workpiece can be categorized: ductile-regime mode (stage I), ductile-to-brittle transition mode (stage II), and brittle mode (stage III).

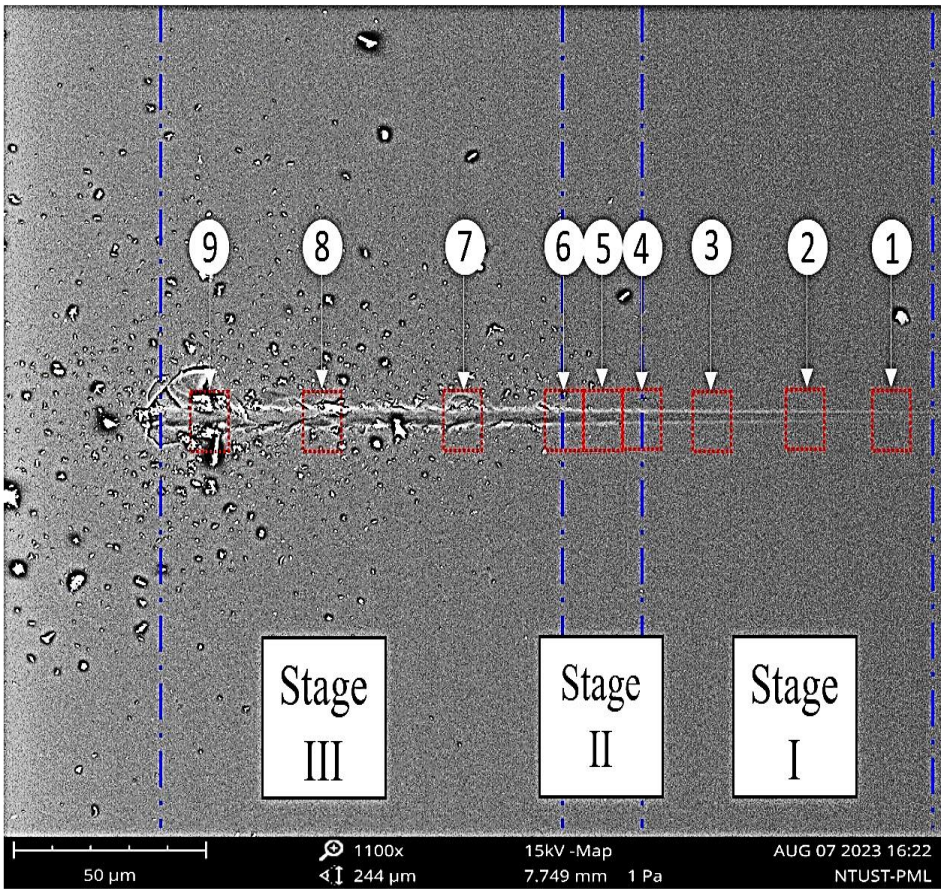

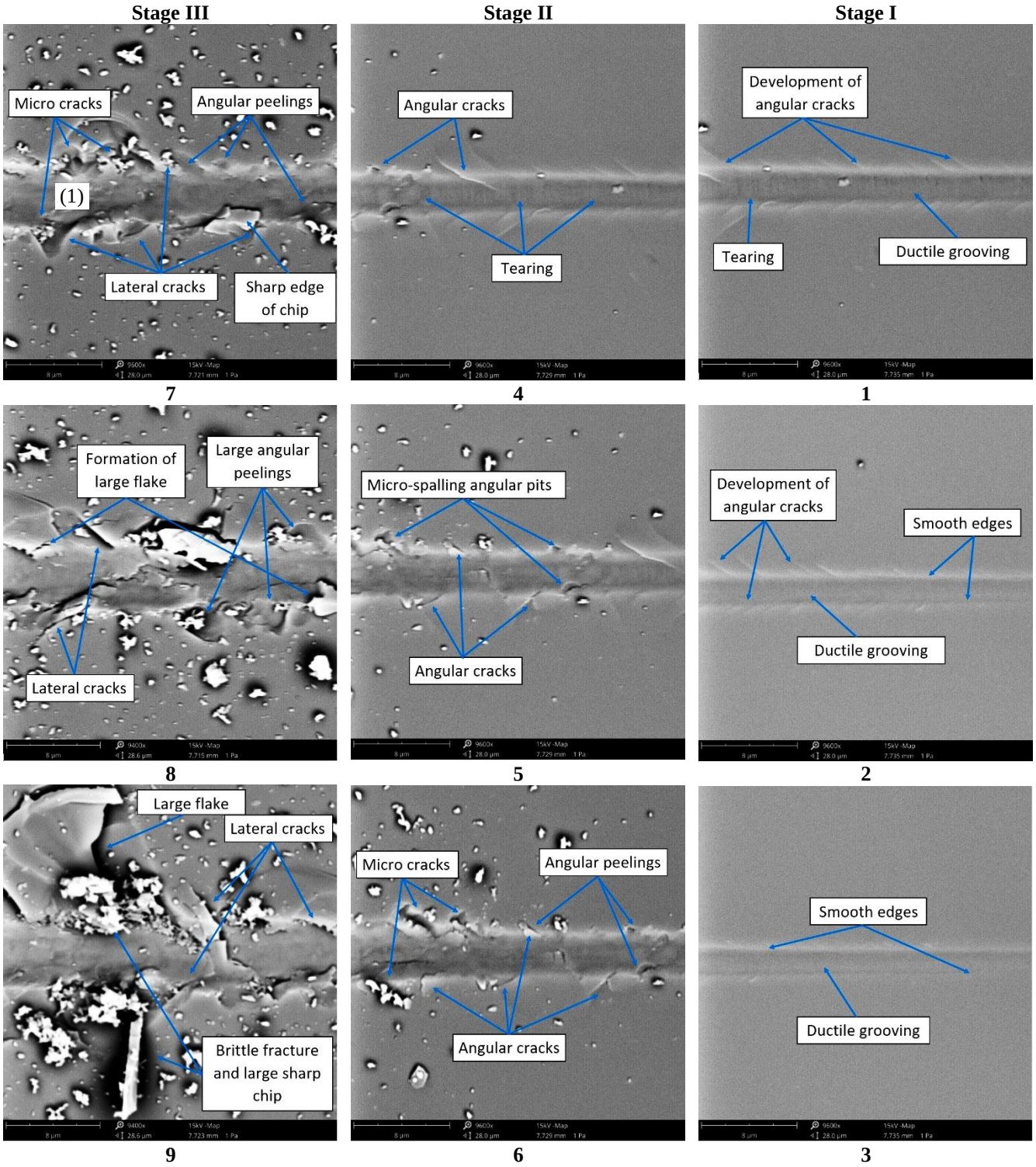

Fig. 2 The observation of scratched groove by SEM micrograph images

• At stage I, the smooth scratching surface is observed at the groove and edge from position 1 to position 3 of the enlarged SEM surface morphology images. Notably, the surface of the groove exhibits distinct plastic flow ripples, devoid of any breaks, and relatively limited penetration along the scratching groove.

According to these observations, it is evident that the results are in strong agreement with the surface deformation structure described by Wu et al. and Kumar et al. during scratching monocrystalline silicon wafers, as well as confirming that the workpiece undergoes removal at ductile regime scratching mode [25, 26].

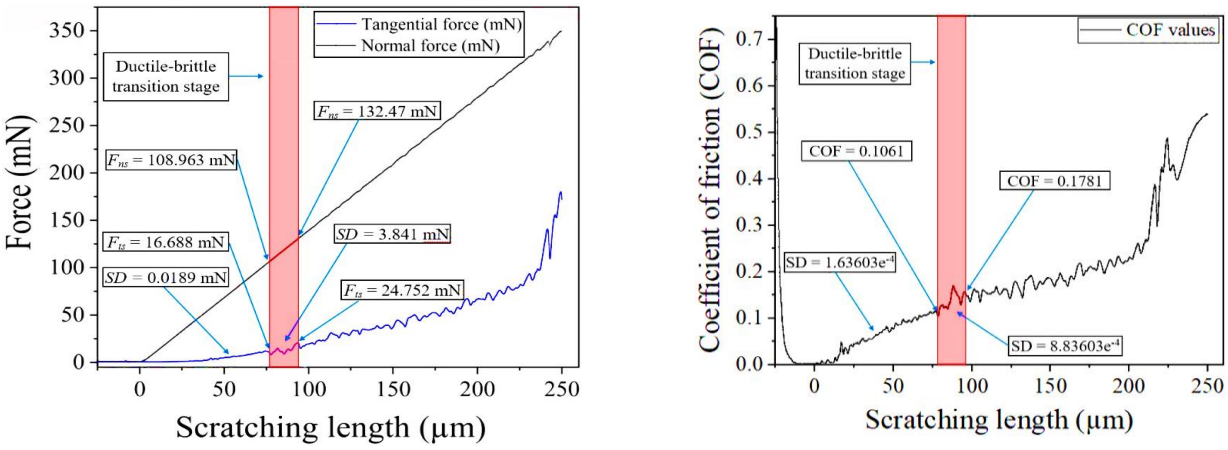

Fig. 3 Results analysis of the F_{ts} and COF along the scratching length.

• At stage II, there are distinct differences between flow ripples under plastic deformation at stage I and transverse angular cracks with tearing curves in the scratched groove at stage II. A remarkable characteristic of these tears is that they occur perpendicular to the diamond tip's motion, resulting from residual stress generated by the scratching experiment. Furthermore, there are formulations for micro-peeling at the angle of the scratching groove. These findings from the micrographs of scratching groove and crack shape, in conjunction with studies on the brittle material transition in nanoscratching by Berkovick and the conical diamond tip of brittle material by Li et al., provide evidence to support the conclusion that this stage represents the transition characteristic between ductile-regime scratching mode and brittle-regime scratching mode silicon, which occurs from position 4 to position 6 [27, 28].

• At stage III, the fracture surface topography and lateral cracks become more noticeable along the edge and inner surface of the groove as it moves from position 7 to position 9. There is a high density of lateral cracks and ductile material ploughing evident from the scratched grooves. Moreover, the predominant fracture modes of the monocrystalline silicon workpiece are brittle fracture and large fracture. These discoveries align with the findings previously documented by Chai et al. and Gu et al., based on scratching with Berkovick diamond tips in 4H-SiC and monocrystalline sapphire, which indicate that brittle removal is the predominant mechanism for material removal [29-31].

For the purpose of accurately identifying the transition point of ductile-to-brittle where the initial brittle fracture, followed by discrete brittle fractures, and ultimately the dominant brittle fracture occurs, this study employs the topography of the scratch groove in conjunction with force signals and coefficient of friction (COF) data obtained from the scratching experiment. The experimental results, presented in Figure 3, clearly show that both the magnitudes of tangential force (Fts) and COF increase with the rise in normal force (Fns) during the scratching experiment. At the initial position to scratching length of 76.54 μm and normal force below Fns = 108.963 mN, both curves of Fts and COF demonstrate a linear increase with Fts ranging from 0 to 16.688 mN with a standard deviation (SD) equal to 0.0189 mN depended on results analysis of Origin software, and for COF, the range is between 0 and 0.1061 with standard deviation of 1.63603e-4. These findings are in excellent agreement with SEM observations of the region exhibiting smooth scratching patterns during stage I, which corresponds to the material is removed in ductile mode. As normal force is increased beyond 76.54 mN, fluctuations become more apparent in both Fts and COF. The signal magnitudes oscillate between 16.688 mN and 24.752 mN with a standard deviation is 3.841 mN for Fts, and between 0.1061 and 0.1781 with a standard deviation is 8.83603e-4 for COF. Based on these observations, the first brittle fracture occurs at a position of 76.54 μm and a normal force of 108.963 mN, which is identified as the transition point. This critical point aligns well with around position 5 in stage II of the transition phase, as evidenced by the SEM image.

3. Experimental Details of Fixed Diamond Abrasive Wire Sawing Process

3.1. Experimental Method

The specific cutting energy obtained in Section 2.2, representing the transition point from ductile to brittle, can be utilized as a criterion in this investigation to ascertain the mechanism by which material is removed during the fixed diamond wire saw operation on a monocrystalline silicon ingot. Specific energy (e) at the transition point of the scratching experiment is determined by dividing the applied scratching force by the unit volume of removed material, as represented by Equation (1). [32, 33]

$$e = \frac{F_{ts}}{A_{groove}} \quad (1)$$

Here, F_{ts} denotes the cutting force at the transition point of monocrystalline silicon under the scratching experiment. At the same time, A_{groove} represents the projected area of the groove on the perpendicular face with respect to the scratching direction at a transition point. The residual morphology of the scratching length is illustrated in Figure 4 (a), with precise measurements carried out using a laser confocal scanning microscope LEXT OLS4000 (Olympus, Inc., Japan) equipped with a 100x magnification objective lens. As illustrated in Figure 4 (b), Mountain 9 (Digital surf) software is utilized for image analysis of measurement cross-section to calibrate the projected area (Agroove) accurately. Figure 4 (c) shows the highlighted projected area with grey-coloured area at the ductile-to-brittle transition point. The theoretical model of the fixed diamond wire sawing experiment is depicted in Figure 5 (a) and Figure 5 (b), showing the diamond abrasive wire driven by a guide roller with reciprocating motion at a velocity (v_w) and feed motion of the ingot at a velocity (v_f).

Due to the wire's flexibility, it deflects during the sawing process, resulting in a bow angle (α). The theoretical model also shows the wire tension (T) during sawing and the distance between guide roller centers (L). The mechanism of the fixed diamond abrasive wire sawing process is considered to be two-body grinding between abrasive and workpiece, as illustrated in Figure 5 (c).

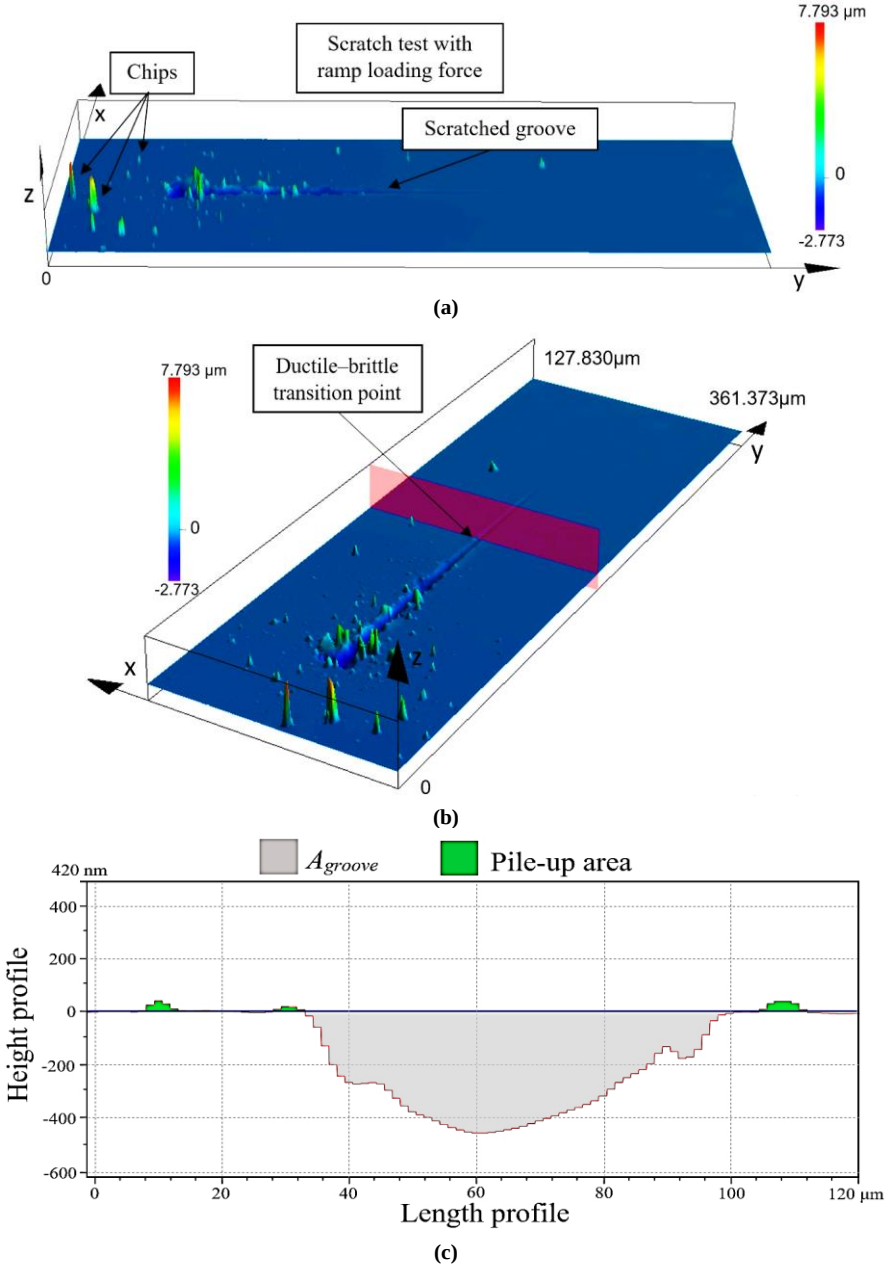

Fig. 4 Scratching surface morphology and image processing to calibrate projected area at a ductile-to-brittle transition point.

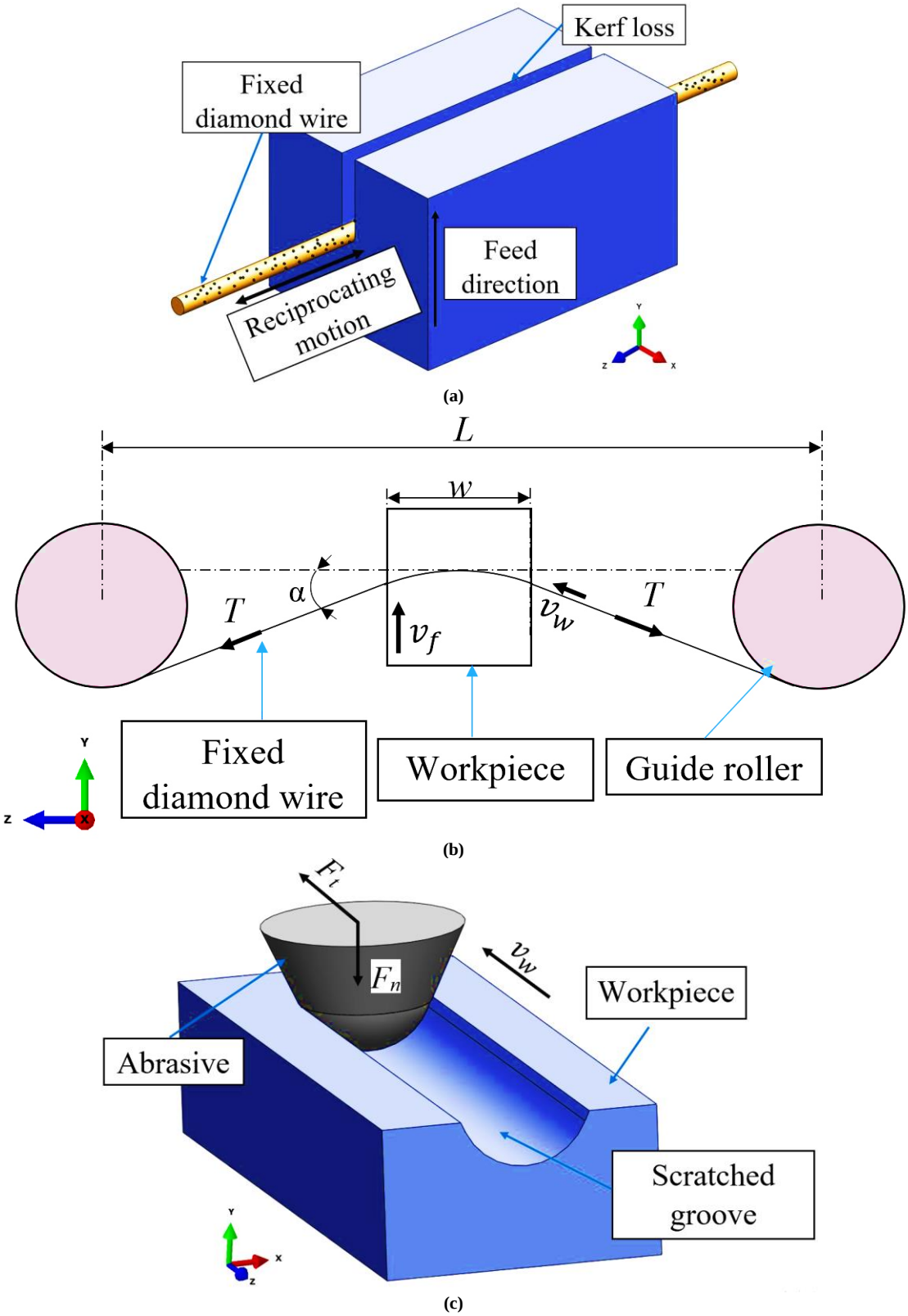

Fig. 5 The schematic diagram of slicing material with fixed abrasive diamond abrasive wire.

Table 1. Design of parameters for fixed diamond abrasive wire sawing process.

Description	Parameters
Coolant	DI water
Spacing between two rollers center	350 mm
Fixed diamond abrasive wire velocity	10 m/s
Workpiece feed velocity (mm/min)	0.02 – 0.04 – 0.052 – 0.06 – 0.08

In order to achieve a certain sawing in the ductile-regime mode in the case of semiconductor materials, especially for a monocrystalline silicon ingot, the specific cutting energy value of a single abrasive must be greater than the specific cutting energy value at the transition point of the monocrystalline silicon ingot so that high-quality finishing of as-sawn wafers can be achieved without brittle fractures. This specific sawing energy (U) is calibrated using Equation (2) [34].

$$U = \frac{P}{Q} = \frac{F_t.v_w}{v_f.\mathrm{b.w}} \quad (2)$$

Here, P represents the consumed energy in the sawing process, calculated as $P = \sum(F_t).v_w$, where $\sum(F_t)$ denotes the total amount of tangential force applied to the abrasives. Q denotes the volume of material removal during the sawing process, determined by $Q = v_f.w.b$, where w and b, respectively, denote the length of the cutting and the breadth of the slit on the specimen. The cutting length of the specimen during the sawing process is determined in this study to have a bow angle of 1 degree, as indicated by the research of Möller et al. [35, 36].

Finally, specific cutting energy is calculated by dividing the total specific sawing energy by the density of the abrasive involved in the sawing process.

3.2. Experiment Details

In this study, the multi-wire sawing machine DWS-600 (Setec Co., Ltd) is utilized for the diamond wire sawing process. Based on Equation (2) of the specific sawing energy function, the feed velocity of the workpiece and the velocity of the fixed diamond abrasive wire are the two critical input parameters that impact the performance of the as-sawn wafers for the purpose of studying the effect of specific sawing energy on the sawing process of a monocrystalline silicon ingot. The feed velocities utilized in this investigation were varied from 0.02 mm/min to 0.08 mm/min with a consistent increment of 0.02 mm/min. Specifically, the transitional feed velocity at the sawing process, which facilitates the removal of ductile-to-brittle material, was calibrated at 0.052 mm/min, as illustrated in Section 3.1. The wire velocity remains unchanged to reduce the incidence of wire breaks and minimize the effect of vibration caused by acceleration during the reciprocating motion of the guide rollers. In the sawing experiments, the fixed diamond abrasive wire moves in a straight vertical direction, whereas the monocrystalline silicon workpiece is securely positioned on a glass substrate between two guide rollers and fed horizontally by the lifting table.

Furthermore, deionized (DI) water is used as the coolant for the sawing process to maintain a controlled temperature and prevent thermal damage. The as-sawn surface of the monocrystalline silicon workpiece has a crystal orientation of (100), and the feed direction along <011> is sliced into three as-sawn wafer specimens with a thickness of 350 μm for each value of the feed velocity. Table 1 presents a detailed overview of the important factors in the experimental design of the sawing processes. These factors are essential for comprehending the effect of feed velocity on the specific sawing energy and its consequences on the material removal mechanism in the sawing processes.

To ensure the integrity of the study's results, it is essential to consistently utilize new fixed abrasive diamond wire during all sawing experiments, thus minimizing any potential influence from worn diamond wires. To accomplish this, a commercially available fixed abrasive diamond wire (Asahi Diamond Industrial., Japan) with a nickel-plated coating, which enhances the holding strength of diamond abrasives, is selected as the sawing tool for these experiments. In Figure 6, SEM images of the surface topography of the fixed diamond wire are presented.

Furthermore, Table 2 provides detailed specifications and parameters of the diamond wire used in the experiments, enabling a comprehensive understanding of its properties and capabilities. These meticulous considerations regarding the diamond abrasive wire selection and its detailed characteristics contribute to the reliability and accuracy of the experimental results in studying the sawing process of monocrystalline silicon workpieces.

Table 2. Specifications of fixed diamond abrasive wires

Parameters	Values
Type of abrasive	Diamond abrasive with nickel coating
Diameter of fixed diamond abrasive wire	160 μm
Surface abrasive distribution density	60 grits/mm^2
Average protruding height of abrasive	12.5 μm
Diamond abrasive size (including nickel layer)	28-35 μm

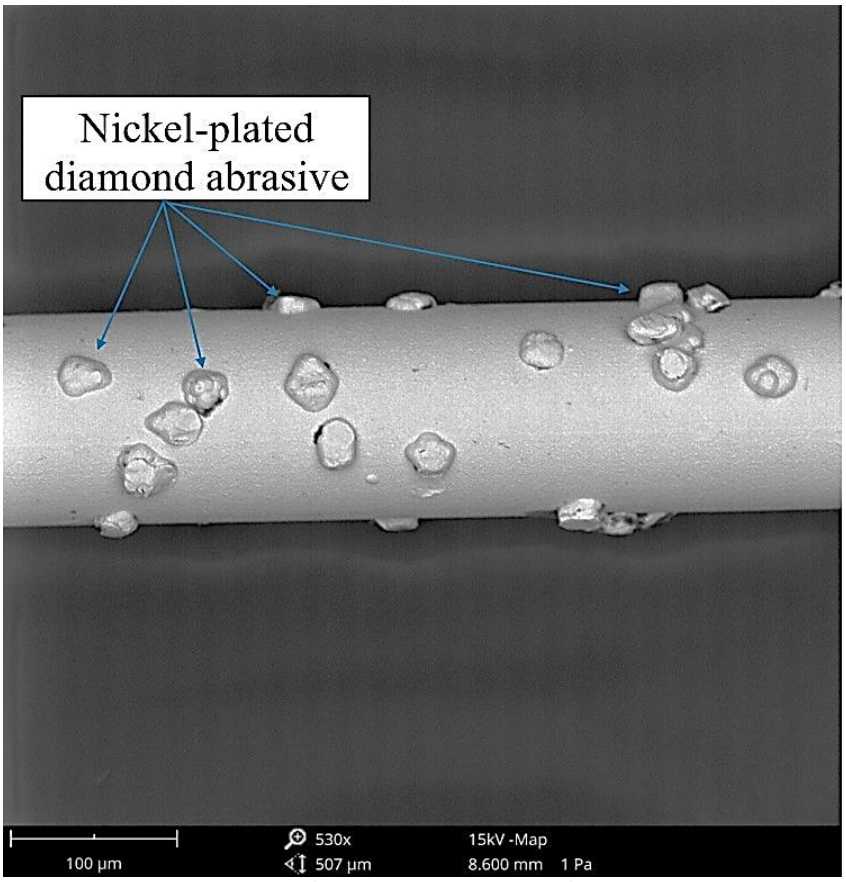

Fig. 6 SEM images of diamond abrasive wire surface morphology.

4. Experimental Results and Discussion

4.1. Surface Morphology

After the sawing operation, the workpiece is heated to melt the adhesive, separated, and then ultrasonically cleaned in DI water for 5 minutes prior to the examination processes of the wafer's surface morphology as-sawn.

The study involves analyzing the surface properties of as-sawn wafer samples using SEM images to understand how the feed velocity affects the material removal processes during the sawing process of a monocrystalline silicon ingot. Figure 7 illustrates the representative SEM images of the surface morphology of as-sawn wafer specimens based on 5 sets of different feed velocities. Consequently, it is evident that an increase in feed velocity from 0.02 mm/min to 0.08 mm/min results in a greater quantity and larger dimensions of brittle pockets when the sawing condition remains constant, and a continuous brittle fracture morphology is generated over a large area. Analyzing SEM images makes it possible to classify as-sawn wafer specimens into three distinct types based on surface morphology characteristics.

Category I: As-sawn wafer surface morphology is characterized by smooth ductile grooves with a few micro pits.

Category II: Surface morphology of as-sawn wafers have a combination of smooth scratching grooves and micro brittle pits.

Category III: As-sawn wafer surface morphology is characterized by extensive crater formations and a large number of brittle fracture zones.

• Category I: Upon observing the surface of the as-sawn wafer specimens at feed velocities of 0.02 mm/min and 0.04 mm/min, slight variations in their surface morphologies are detected, as depicted in Figure 7 (a) and Figure 7 (b). The predominant material removal mechanism is characterized by smooth ductile grooves accompanied by a few micro-pits with measuring sizes from 1 µm to 2 µm on the as-sawn wafers surface morphology. Additionally, a flowing plastic ripple can be seen in regions where the cutting trajectories are highly overlapping, and the number of micro-pits occurs at a feed velocity of 0.04 mm/min with a higher density than that at a feed velocity of 0.02 mm/min. However, the size of these pits remains constant, and they are shallow. According to the surface morphology of these observations, the sawing processes indicate that they are sawn in the ductile-regime mode region, which is in agreement with the surface morphology assessments made by Costa et al. and Gao et al. on the monocrystalline silicon as-sawn wafer surface [37, 38].

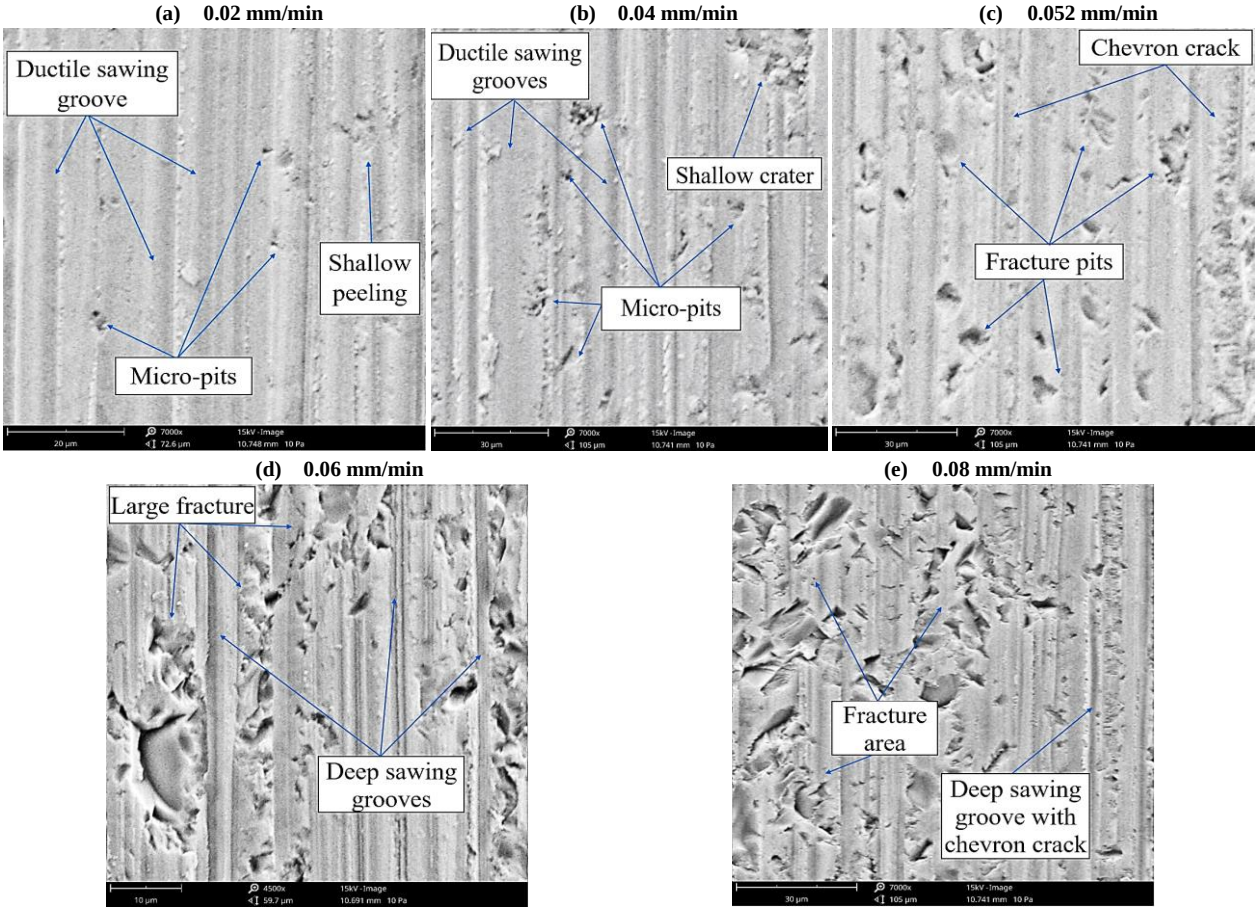

Fig. 7 SEM micrograph images of a monocrystalline silicon as-sawn wafer surface morphology under changing feed velocities (a) 0.02 mm/min, (b) 0.04mm/min, (c) 0.052mm/min, (d) 0.06mm/min, and (e) 0.08 mm/min

• Category II: When the setup of the feed velocity at transition-specific sawing energy of 0.052 mm/min, there appeared random large diameter brittle crack pits emerged along the movement direction of the fixed diamond wire, causing interruptions in the linear, smooth ductile zone along the sawing direction. Additionally, multiple consecutive chevron cracks are visible inside the ductile groove. The as-sawn wafer surface begins to show growth in the length of lateral cracks in conjunction with an increase in the size of micro pits, which can reach up to 15 μm, as illustrated in Figure 7 (c). Following a thorough evaluation of the as-sawn wafer surface topography in conjunction with the findings reported in the references [39, 40], The material removal mechanism during the sawing process of monocrystalline silicon is determined to transition progressively from ductile mode to a critical condition of mixed ductility and brittleness removal.

• Category III: In the case of feed velocity exceeding feed velocity at transition-specific sawing energy of 0.052 mm/min, the as-sawn wafer surfaces are dominated by a random distribution of brittle fractures, and numerous brittle cracks interlaced with each other, which makes the surface an adjacent craterlike morphology, as illustrated in Figure 7 (d) and Figure 7 (e). Besides that, it is also evident that some long, deep sawing grooves had been formed due to large cutting forces. In accordance with surface morphological analyses of as-sawn wafers, it confirms that the removal mechanism of material is predominantly brittle mode, which is also in good agreement with the estimation determined by the results of cutting groove profile during machining brittle material by [28] and [41].

4.2. Subsurface Damage

To estimate the effect of the feed velocity material removal mechanism during the sawing process, the depth of micro-cracks within the subsurface damage layer of as-sawn wafers is measured in this section using a focused ion beam (FIB) measurement instrument (Quanta 3D FEG, FEI, Netherlands). The subsurface crack depth of as-sawn wafers at each feed velocity is measured at nine locations with uniform distribution on the surface of specimens, and average values are utilized to determine the final subsurface damage values. Figure 8 shows the comparison of the values of subsurface damage and the representative SEM images of subsurface damage of the as-sawn wafers at different feed velocity values.

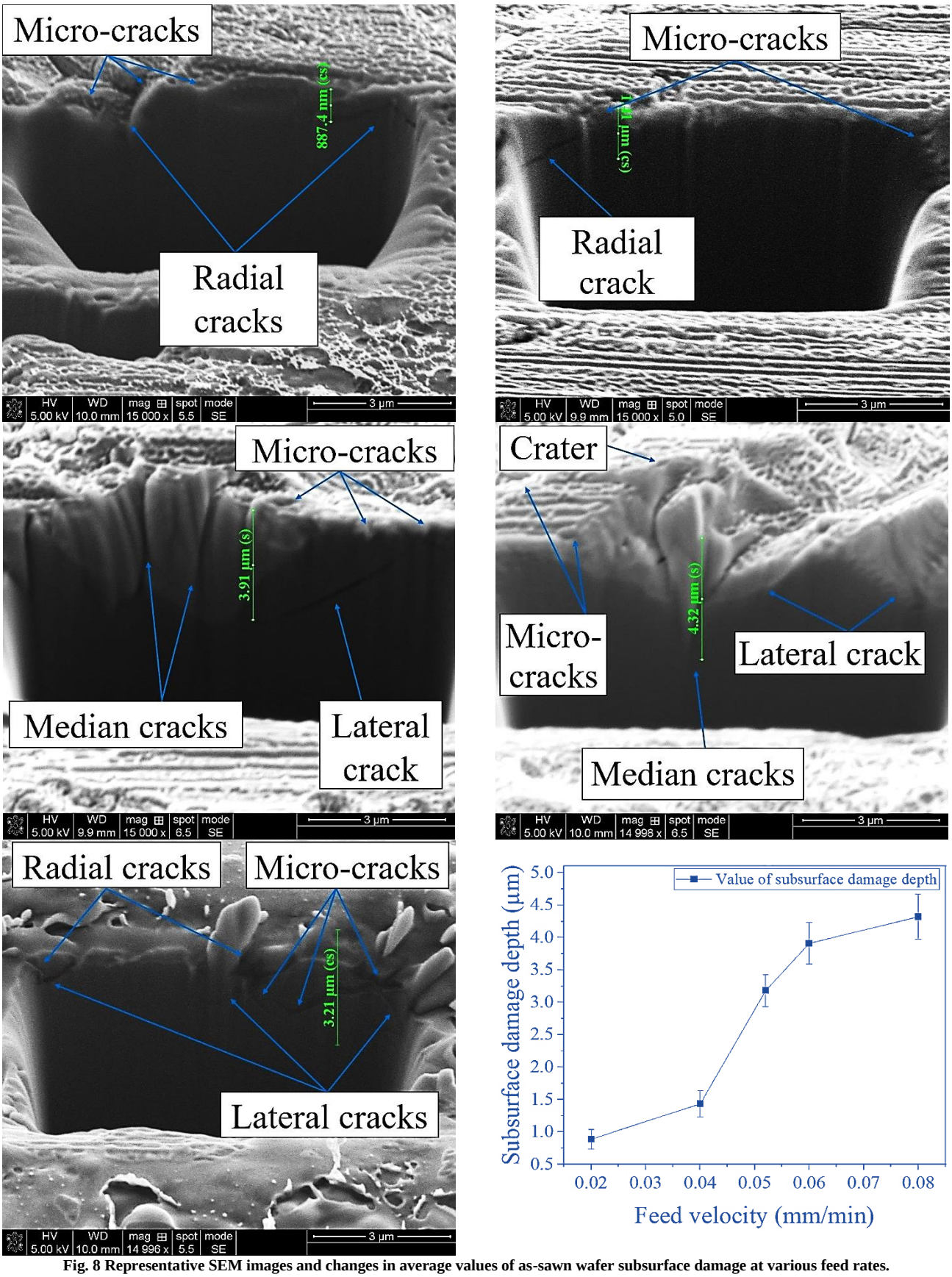

Fig. 8 Representative SEM images and changes in average values of as-sawn wafer subsurface damage at various feed rates.

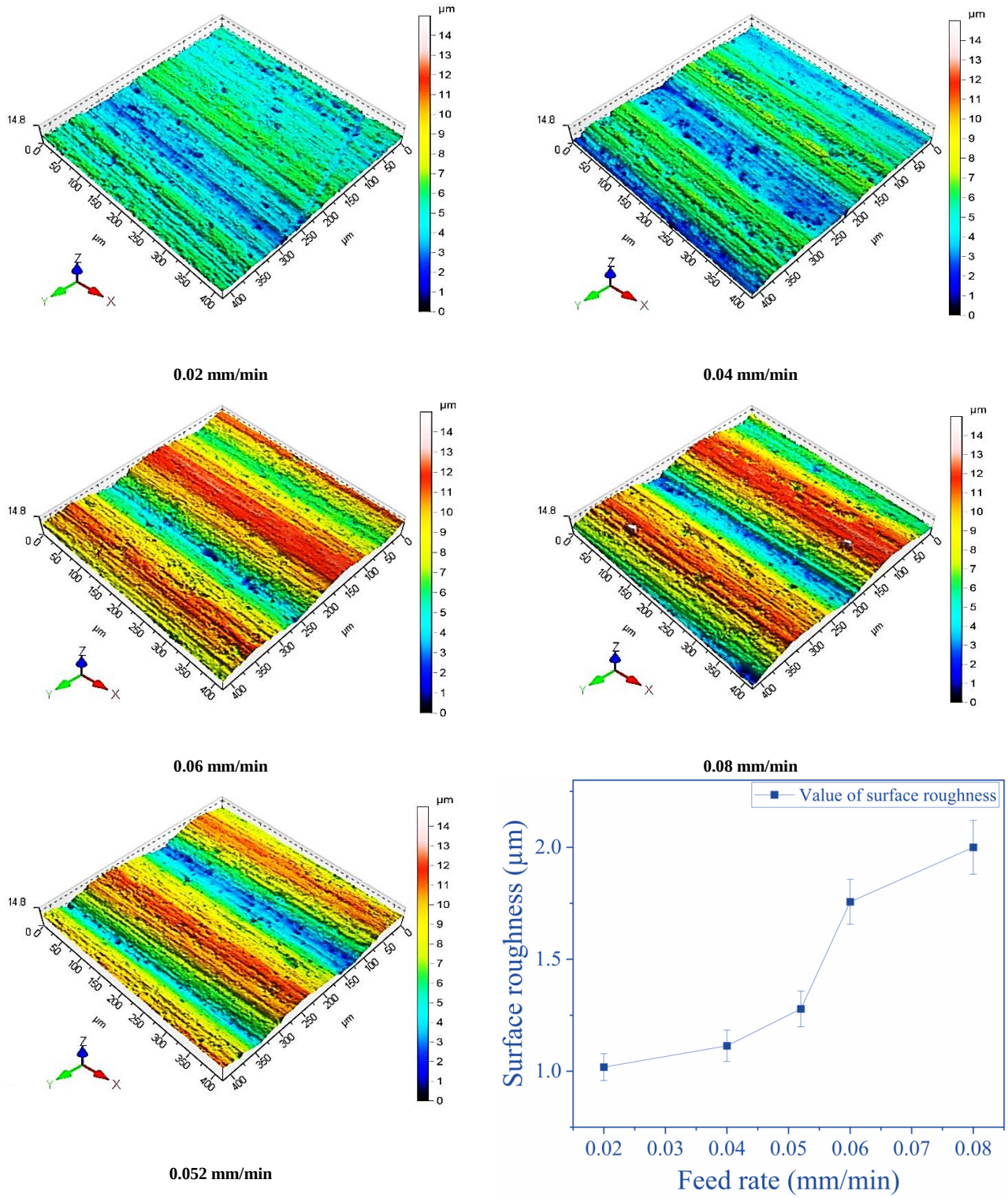

Fig. 9 Changing values of average surface roughness with increasing feed rate.

The measurement results indicate that the depth of subsurface damage increases with the increment in the feed velocity of the workpiece. Specifically, as the feed velocity increases from 0.02 mm/min to 0.04 mm/min, the average subsurface damage values exhibit a slight increase. This can be attributed to the fact that increasing feed velocities lead to diamond abrasives applying larger normal forces to the workpiece, thereby increasing the normal sawing force of the

fixed abrasive diamond and resulting in elevated subsurface damage values within the monocrystalline silicon during the sawing process. Nevertheless, at these velocities, the specific sawing energy remains higher than the specific sawing energy at the ductile-to-brittle transition point, signifying that the sawing process continues to be conducted in the ductile mode. The micro-cracks observed within the subsurface of as-sawn wafers at these velocities are primarily radial cracks and micro-cracks aligned parallel to the direction of the sawing groove. At the feed velocity equal to the transition feed velocity of 0.052 mm/min, in the subsurface, the lateral cracks begin to appear with a mean depth of 3.15 μm in combination with numerous micro-cracks. The depth and number of micro-cracks at the feed velocity of 0.052 mm/min are substantially greater than those at a feed velocity of 0.04 mm/min.Moreover, these lateral cracks are interconnected with micro-cracks and radial micro-cracks, exhibiting relatively greater depth, and the lateral cracks tend to produce shallow chipping of the wafer surface. When the feed velocity exceeds the transition feed velocity, the subsurface damage predominantly consists of median cracks. Furthermore, at these feed velocities, the median cracks concentrate at the saw mark positions, and there are instances of bifurcations around median cracks. This inclined crack geometry increases the likelihood of fracture during subsequent handling and processing operations.

4.3. Surface Roughness

In order to obtain surface roughness measurements of as-sawn wafer specimens for each feed velocity condition, an optical non-contact Coherence Correlation Interferometry (CCI) measurement was employed at nine locations across the specimens' surfaces in a uniform distribution, and the final values of measurements are determined as average values. According to the measurement data, the arithmetic averages of surface roughness in three dimensions (S_a) in an as-sawn wafer surface profile following the feed velocity direction are analyzed with Taylor Map 6.0 software according to ISO 25178. Based on the change in feed velocity values, Figure 9 shows the variation in average values and deviations of S_a. In cases where the feed velocity of the workpiece is lower than the transition feed velocity of 0.052 mm/min at ductile-to-brittle material removal mechanism during sawing process, the average values of Sa slightly increase from 1.0185±0.061 μm at feed velocity of 0.02 mm/min to 1.1137±0.077 μm at feed velocity of 0.04 mm/min. This is mainly because the normal force exerted by diamond abrasives on the workpiece at these feed velocities is smaller than the normal force at the ductile-to-brittle transition point of monocrystalline silicon. This causes a greater number of abrasives to remove material in a ductile-regime mode, resulting in the formation of parallel channels along the sawing direction. In the case of feed velocity greater than transition feed velocity, the average values of S_a sharply increase from 1.2785±0.086 μm at feed velocity of 0.052 mm/min to 2.05±0.12 μm at feed velocity of 0.08 mm/min. This occurs because the cutting force acting on the cutting area exceeds the normal force at which monocrystalline silicon transitions from ductile to brittle, which leads to the abrasive removal material being transformed into brittle mode. The increase in depth of brittle crack pits along the direction of the sawing grooves and the large volume of crater area appear with the high density on as-sawn wafers surface morphology, which results in increased surface roughness values.

5. Conclusion

This study introduces a new method for achieving the ductile regime mode during the fixed diamond wire sawing process based on calibrated specific cutting energy at the ductile-brittle transition point. Furthermore, this study provides a comprehensive account of the methodologies and experimental references employed to assess the as-sawn wafer surface morphology throughout the fixed diamond abrasive wire sawing procedure.

These findings lead to the following conclusions:

1. The position of the ductile-to-brittle transition point of monocrystalline silicon can be accurately determined by combining signal analysis from the scratching experiment with image analysis of SEM micrographs.
2. The specific cutting energy of monocrystalline silicon at the transition point of ductile-to-brittle can be applied to a wide variety of machining processes to achieve a ductile regime machining process.
3. The quality of the as-sawn wafer surface of monocrystalline silicon ingots, such as roughness, morphology, and subsurface damage, is assessed using a commercial testing device, which enables estimation of the influence of specific sawing energy parameters in the diamond abrasive wire sawing process.
4. Fixed diamond abrasive wire sawing process in ductile regime mode of monocrystalline silicon ingot can be achieved by adjusting feed velocity based on specific cutting energy in order to produce an as-sawn wafer with a smooth scratching groove, no subsurface damage, and crack-free.
5. By determining the attainment of the ductile regime mode of monocrystalline silicon ingot in conjunction with control feed velocity, this study's findings suggest that future research can concentrate on simulating and modeling the impact of diamond abrasive shape and diamond abbreviate properties on the surface morphology of as-sawn wafers. This would enable a more comprehensive examination of the influence that diamond shape has on the surface morphology of as-sawn wafers.

Acknowledgments

The authors acknowledge the support of time and facilities from Tra Vinh University (TVU) for this study.

References

[1] Patrick Campbell, and Martin A. Green, "High Performance Light Trapping Textures for Monocrystalline Silicon Solar Cells," *Solar Energy Materials and Solar Cells*, vol. 65, no. 1-4, pp. 369-375, 2001. [CrossRef] [Google Scholar] [Publisher Link]

[2] Nathalie da Silva Cavalcanti Monteiro et al., "Brazil Market Outlook for Photovoltaic Solar Energy: A Survey Study," *British Journal of Applied Science & Technology*, vol. 21, no. 5, pp. 1-11, 2017. [CrossRef] [Google Scholar] [Publisher Link]

[3] Xuegong Yu et al., "Thin Czochralski Silicon Solar Cells Based on Diamond Wire Sawing Technology," *Solar Energy Materials and Solar Cells*, vol. 98, pp. 337-342, 2012. [CrossRef] [Google Scholar] [Publisher Link]

[4] Bruno Ceccaroli, Eivind Ovrelid, and Sergio Pizzini, *Solar Silicon Processes: Technologies, Challenges, and Opportunities*, Boca Raton, USA: CRC Press, pp. 1-272, 2016. [CrossRef] [Google Scholar] [Publisher Link]

[5] Kazuaki Tomono et al., "Recycling of Kerf Loss Silicon Derived from Diamond-Wire Saw Cutting Process by Chemical Approach," *Separation and Purification Technology*, vol. 120, pp. 304-309, 2013. [CrossRef] [Google Scholar] [Publisher Link]

[6] N. Watanabe et al., "Characterization of Polycrystalline Silicon Wafers for Solar Cells Sliced with Novel Fixed-Abrasive Wire," *Progress in Photovoltaics: Research and Applications*, vol. 18, no. 7, pp. 485-490, 2010. [CrossRef] [Google Scholar] [Publisher Link]

[7] B. Meinel et al., "Comparison of Diamond Wire Cut and Silicon Carbide Slurry Processed Silicon Wafer Surfaces after Acidic Texturisation," *Materials Science in Semiconductor Processing*, vol. 26, pp. 93-100, 2014. [CrossRef] [Google Scholar] [Publisher Link]

[8] L.J. Vandeperre et al., "The Hardness of Silicon and Germanium," *Acta Materialia*, vol. 55, no. 18, pp. 6307-6315, 2007. [CrossRef] [Google Scholar] [Publisher Link]

[9] Han Huang et al., "Science and Art of Ductile Grinding of Brittle Solids," *International Journal of Machine Tools and Manufacture*, vol. 161, 2021. [CrossRef] [Google Scholar] [Publisher Link]

[10] D. Axinte et al., "On the Influence of Single Grit Micro-Geometry on Grinding Behavior of Ductile and Brittle Materials," *International Journal of Machine Tools and Manufacture*, vol. 74, pp. 12-18, 2013. [CrossRef] [Google Scholar] [Publisher Link]

[11] T.P. Leung, W.B. Lee, and X.M. Lu, "Diamond Turning of Silicon Substrates in Ductile-Regime," *Journal of Materials Processing Technology*, vol. 73, no. 1-3, pp. 42-48, 1998. [CrossRef] [Google Scholar] [Publisher Link]

[12] P.S. Sreejith, and B.K.A. Ngoi, "Material Removal Mechanisms in Precision Machining of New Materials," *International Journal of Machine Tools and Manufacture*, vol. 41, no. 12, pp. 1831-1843, 2001. [CrossRef] [Google Scholar] [Publisher Link]

[13] Sofia H. Vanger, *Silicon Carbide: New Materials, Production Methods & Applications*, Nova Publishers, vol. 141-167, 2011. [Google Scholar] [Publisher Link]

[14] W.S. Blackley, and R.O. Scattergood, "Chip Topography for Ductile-Regime Machining of Germanium," *Journal of Engineering for Industry*, vol. 116, no. 2, pp. 263-266, 1994. [CrossRef] [Google Scholar] [Publisher Link]

[15] B.V. Tanikella et al., "Phase Transformations During Microcutting Tests on Silicon," *Applied Physics Letters*, vol. 69, no. 19, pp. 2870-2872, 1996. [CrossRef] [Google Scholar] [Publisher Link]

[16] Deepak Ravindra, and John Patten, "Ductile Regime Single Point Diamond Turning of Quartz Resulting in an Improved and Damage-Free Surface," *Machining Science and Technology*, vol. 154, no. 4, pp. 357-375, 2011. [CrossRef] [Google Scholar] [Publisher Link]

[17] J.H. Giovanola, and I. Finnie, "On the Machining of Glass," *Journal of Materials Science*, vol. 15, pp. 2508-2514, 1980. [CrossRef] [Google Scholar] [Publisher Link]

[18] K.E. Puttick et al., "Single-Point Diamond Machining of Glasses," *Proceedings of the Royal Society A, Mathematical, Physical and Engineering Science*, vol. 426, no. 1870, pp. 19-30, 1989. [CrossRef] [Google Scholar] [Publisher Link]

[19] Siva Venkatachalam, Xiaoping Li, and Steven Y. Liang, "Predictive Modeling of Transition Undeformed Chip Thickness in Ductile-Regime Micro-Machining of Single Crystal Brittle Materials," *Journal of Materials Processing Technology*, vol. 209, no. 7, pp. 3306-3319, 2009. [CrossRef] [Google Scholar] [Publisher Link]

[20] Takaaki Suzuki, Yuki Nishino, and Jiwang Yan, "Mechanisms of Material Removal and Subsurface Damage in Fixed-Abrasive Diamond Wire Slicing of Single-Crystalline Silicon," *Precision Engineering*, vol. 50, pp. 32-43, 2017. [CrossRef] [Google Scholar] [Publisher Link]

[21] Yufei Gao, Peiqi Ge, and Tengyun Liu, "Experiment Study on Electroplated Diamond Wire Saw Slicing Single-Crystal Silicon," *Materials Science in Semiconductor Processing*, vol. 56, pp. 106-114, 2016. [CrossRef] [Google Scholar] [Publisher Link]

[22] Liyuan Wang et al., "Analytical Prediction of Subsurface Microcrack Damage Depth in Diamond Wire Sawing Silicon Crystal," *Materials Science in Semiconductor Processing*, vol. 112, 2020. [CrossRef] [Google Scholar] [Publisher Link]

[23] Yan Wang et al., "Theoretical Study on Sawing Force of Ultrasonic Vibration Assisted Diamond Wire Sawing (UAWS) Based on Abrasives Wear," *Wear*, vol. 496-497, 2022. [CrossRef] [Google Scholar] [Publisher Link]

[24] Craig W. Hardin, Jun Qu, and A.J. Shih, "Fixed Abrasive Diamond Wire Saw Slicing of Single-Crystal Silicon Carbide Wafers," *Materials and Manufacturing Processes*, vol. 19, no. 2, pp. 355-367, 2007. [CrossRef] [Google Scholar] [Publisher Link]

[25] Hao Wu, and Shreyes N. Melkote, "Effect of Crystallographic Orientation on Ductile Scribing of Crystalline Silicon: Role of Phase Transformation and Slip," *Materials Science and Engineering: A*, vol. 549, pp. 200-205, 2012. [CrossRef] [Google Scholar] [Publisher Link]

[26] Arkadeep Kumar et al., "Effect of Wear of Diamond Wire on Surface Morphology, Roughness and Subsurface Damage of Silicon Wafers," *Wear*, vol. 364-365, pp. 163-168, 2016. [CrossRef] [Google Scholar] [Publisher Link]

[27] Xuliang Li et al., "Brittle-to-Ductile Transition in Nanoscratching of Silicon and Gallium Arsenide Using Berkovich and Conical Tips," *Applied Surface Science*, vol. 637, pp. 1-12, 2023. [CrossRef] [Google Scholar] [Publisher Link]

[28] Xinying Li et al., "Nucleation Location and Propagation Direction of Radial and Median Cracks for Brittle Material in Scratching," *Ceramics International*, vol. 45, no. 6, pp. 7524-7536, 2019. [CrossRef] [Google Scholar] [Publisher Link]

[29] Peng Chai et al., "Study on Damage of 4H-SiC Single Crystal through Indentation and Scratch Testing in Micro-Nano Scales," *Applied Sciences*, vol. 10, no. 17, pp. 1-16, 2020. [CrossRef] [Google Scholar] [Publisher Link]

[30] Xingshi Gu et al., "Effect of Cutting Tool Geometries on the Ductile-Brittle Transition of Monocrystalline Sapphire," *International Journal of Mechanical Sciences*, vol. 148, pp. 565-577, 2018. [CrossRef] [Google Scholar] [Publisher Link]

[31] Jiunn-Jyh Junz Wang, and Yong-Yuan Liao, "Critical Depth of Cut and Specific Cutting Energy of a Microscribing Process for Hard and Brittle Materials," *Journal of Engineering Materials and Technology*, vol. 130, no. 1, pp. 1-6, 2008. [CrossRef] [Google Scholar] [Publisher Link]

[32] Min Ji et al., "Investigation of Material Removal Mechanisms and Ductile-Brittle Transition Zone of Zirconia Ceramics Sintered at Various Temperatures," *Journal of the Mechanical Behavior of Biomedical Materials*, vol. 125, 2022. [CrossRef] [Google Scholar] [Publisher Link]

[33] Hui Huang, Yuxing Zhang, and Xipeng Xu, "Experimental Investigation on the Machining Characteristics of Single-Crystal SiC Sawing with the Fixed Diamond Wire," *The International Journal of Advanced Manufacturing Technology*, vol. 81, pp. 955-965, 2015. [CrossRef] [Google Scholar] [Publisher Link]

[34] Ningchang Wang et al., "Research on the Machinability of A-Plane Sapphire Under Diamond Wire Sawing in Different Sawing Directions," *Ceramics International*, vol. 45, no. 8, pp. 10310-10320, 2019. [CrossRef] [Google Scholar] [Publisher Link]

[35] H.J. Möller, "Basic Mechanisms and Models of Multi-Wire Sawing," *Advanced Engineering Materials*, vol. 6, no. 7, pp. 501-513, 2004. [CrossRef] [Google Scholar] [Publisher Link]

[36] Daniel Meißner et al., "Loss of Wire Tension in the Wire Web During the Slurry Based Multi Wire Sawing Process," *Solar Energy Materials and Solar Cells*, vol. 120, pp. 346-355, 2014. [CrossRef] [Google Scholar] [Publisher Link]

[37] Erick Cardoso Costa et al., "Experimental Investigation of the Sawn Surface of Monocrystalline Silicon Cut by Endless Diamond Wire Sawing," *Materials Research*, vol. 23, no. 4, pp. 1-8, 2020. [CrossRef] [Google Scholar] [Publisher Link]

[38] Yufei Gao et al., "Material Removal and Surface Generation Mechanisms in Diamond Wire Sawing of Silicon Crystal," *Materials Science in Semiconductor Processing*, vol. 103, 2019. [CrossRef] [Google Scholar] [Publisher Link]

[39] Uygar Pala, Fredy Kuster, and Konrad Wegener, "Characterization of Electroplated Diamond Wires and the Resulting Workpiece Quality in Silicon Sawing," *Journal of Materials Processing Technology*, vol. 276, 2020. [CrossRef] [Google Scholar] [Publisher Link]

[40] T.G. Bifano, T.A. Dow, and R.O. Scattergood, "Ductile-Regime Grinding: A New Technology for Machining Brittle Materials," *Journal of Manufacturing Science and Engineering*, vol. 113, no. 2, pp. 184-189, 1991. [CrossRef] [Google Scholar] [Publisher Link]

[41] D.B. Marshall, B.R. Lawn, and A.G. Evans, "Elastic/Plastic Indentation Damage in Ceramics: The Lateral Crack System," *Journal of the American Ceramic Society*, vol. 65, no. 11, pp. 561-566, 1982. [CrossRef] [Google Scholar] [Publisher Link]